The catalytic activity of the endoplasmic reticulum-resident protein microsomal epoxide hydrolase towards carcinogens is retained on inversion of its membrane topology

Thomas FRIEDBERG*, Romy HOLLER, Bettina LÖLLMANN, Michael ARAND and Franz OESCH
Institute of Toxicology, University of Mainz, Obere Zahlbacherstrasse 67, D-55131 Mainz, Federal Republic of Germany

Diol epoxides formed by the sequential action of cytochrome *P*-450 and the microsomal epoxide hydrolase (mEH) in the endoplasmic reticulum (ER) represent an important class of ultimate carcinogenic metabolites of polycyclic aromatic hydrocarbons. The role of the membrane orientation of cytochrome *P*-450 and mEH relative to each other in this catalytic cascade is not known. Cytochrome *P*-450 is known to have a type I topology. According to the algorithm of Hartman, Rapoport and Lodish [(1989) Proc. Natl. Acad. Sci. U.S.A. **86**, 5786–5790], which allows the prediction of the membrane topology of proteins, mEH should adopt a type II membrane topology. Experimentally, mEH membrane topology has been disputed. Here we demonstrate that, in contrast with the theoretical prediction, the rat mEH has exclusively a type I membrane topology. Moreover we show that this topology can be inverted without affecting the catalytic activity of mEH. Our conclusions are supported by the observation that two mEH constructs (mEH_{g1} and mEH_{g2}), containing engineered potential glycosylation sites at two separate locations after the C-terminal site of the membrane anchor, were not glycosylated in fibroblasts. However, changing the net charge at the N-terminus of these engineered mEH proteins by +3 resulted in proteins ($^{++}mEH_{g1}$ and $^{++}mEH_{g2}$) that became glycosylated and consequently had a type II topology. The sensitivity of these glycosylated proteins to endoglycosidase H indicated that, like the native mEH, they are still retained in the ER. The engineered mEH proteins were integrated into membranes as they were resistant to alkaline extraction. Interestingly, an insect mEH with a charge distribution in its N-terminus similar to $^{++}mEH_{g1}$ has recently been isolated. This enzyme might well display a type II topology instead of the type I topology of the rat mEH. Importantly, mEH_{g1}, having the natural cytosolic orientation, as well as $^{++}mEH_{g1}$, having an artificial luminal orientation, displayed rather similar substrate turnovers for the mutagenic metabolite benzo[*a*]pyrene 4,5-oxide. To our knowledge this is the first report demonstrating that topological inversion of a protein within the membrane of the ER has only a moderate effect on its enzymic activity, despite differences in folding pathways and redox environments on each side of the membrane. This observation represents an important step in the evaluation of the influence of mEH membrane orientation in the cascade of events leading to the formation of ultimate carcinogenic metabolites, and for studying the general importance of metabolic channelling on the surface of membranes.

INTRODUCTION

The microsomal epoxide hydrolase (mEH; EC 3.3.2.3) plays a central role in the metabolism of several carcinogenic polycyclic aromatic hydrocarbons [1–4] and has been identified as an early preneoplastic antigen [5]. Cytochrome *P*-450 and mEH catalyse in this metabolism a three-step reaction culminating in the formation of dihydrodiol epoxides, which are thought to be the ultimate carcinogenic metabolites of certain polycyclic aromatic hydrocarbons. The role of the membrane topology of cytochrome *P*-450 and mEH in this metabolic cascade is unknown.

MEH is co-translationally inserted into the endoplasmic reticulum (ER); the N-terminus of the protein is not cleaved proteolytically during this process [6,7]. The protein remains mainly in the ER [8]. Recently we were able to demonstrate that mEH has a single membrane-anchor signal sequence located at the N-terminus of the protein [9].

Proteins that span the membrane once can assume either a type I (N_{exo}/C_{cyt}) or a type II (N_{cyt}/C_{exo}) orientation [10]. The membrane orientation of single anchor sequences was highly correlated with the charge difference, δ(C-N), between charged amino acid residues preceding the hydrophobic core of the membrane anchor and charged amino acid residues following this core up to a distance of 10–15 residues on each side [11,12]. In these analyses it was found that a negative charge difference, $\delta(C\text{-}N) < 0$, always correlated with a type II topology. For mEH of human, rat and rabbit the charge differences are −3, −2 and −4 respectively. These values suggest that mEH from these species have exclusively a type II orientation in the membrane of the ER [11]. However, on the basis of labelling experiments with membrane-impermeant protein-reactive fluorescent probes, and on immuno-electron microscopy, there is evidence that the mEH-like cytochrome *P*-450 has a type I membrane orientation [13,14]. If this is correct, the sequence of events catalysed by cytochrome *P*-450 and by mEH, leading to the formation of the ultimate carcinogenic metabolites of polycyclic aromatic hydrocarbons, would take place exclusively at the cytosolic face of the ER, allowing highly efficent metabolic channelling [15]. However, a

Abbreviations used: endo H, endoglycosidase H; ER, endoplasmic reticulum; mEH, microsomal epoxide hydrolase; mEH_{g1}, mEH with an engineered N-glycosylation signal at position 39; mEH_{g2}, mEH with an engineered glycosylation signal at position 303; $^{++}$mEH, mEH in which charges in the N-terminal sequence have been altered by +3; $^{++}mEH_{g1}$, $^{++}$mEH with an engineered N-glycosylation signal at position 39; $^{++}mEH_{g2}$, $^{++}$mEH with an engineered N-glycosylation signal at position 303; δmEH, mEH with a deleted membrane anchor.

* To whom correspondence should be addressed. Present address: Biomedical Research Centre, Ninewells Hospital, Dundee DD1 9SY, Scotland, U.K.

recent report [16] suggested, on the basis of immunological assays and on protease protection experiments, that mEH was able to adopt a type I as well as a type II membrane topology [16]. Interestingly the same group presented evidence that the endogenous mEH of hepatocytes acts as a carrier for bile acids [16,17]. However, we have shown that the heterologously expressed mEH does not act as a carrier for bile acids in fibroblasts [18].

In this report we have tried to define the membrane topology of the rat mEH more precisely. In the course of these studies we also wanted to address the important question of whether or not the catalytic properties of the enzyme are influenced by the differences in the protein-folding environments that have been shown to exist on both sides of the ER membrane. For example, the correct folding of the peptide chain has been shown to be assisted by proteins, termed chaperones, that facilitate folding of nascent proteins. Different types of chaperone are present on the luminal and cytosolic sides of the ER [19]. In addition, protein folding is influenced by the redox environment, which is more oxidizing in the lumen of the ER than in the cytosol [20].

For our experiments we engineered mEH mutants with an altered net charge at the N-terminus and investigated the resulting effects on mEH topology and function. We have shown that the topological inversion of mEH has only a moderate effect on the enzymic properties of the enzyme towards the model mutagen benzo[*a*]pyrene 4,5-oxide. This opens an avenue for studying the role of mEH membrane topology in the formation of ultimate carcinogenic metabolites.

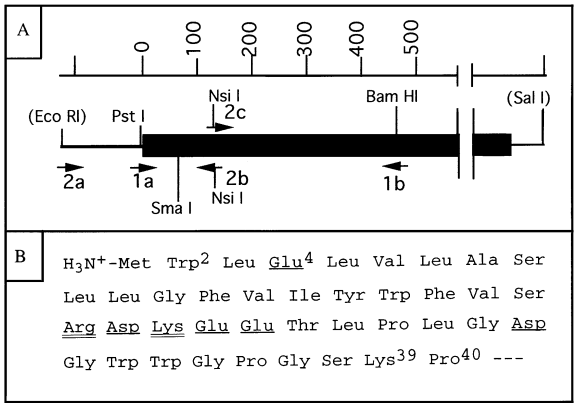

Figure 1 Engineering and sequences of mEH-related proteins

(**A**) Strategy for engineering DNA templates coding for the modified mEH proteins by PCR. The non-coding regions and the coding region of the mEH cDNA are indicated as thick lines and a filled box respectively. The numbering of the scale at the top of the figure starts with the initiation codon of the mEH cDNA. The PCR primers are shown as arrows and their designations are those used in the text. Restriction sites used in the generation of the modified cDNA constructs are shown; those in parentheses are part of the plasmid polylinker. (**B**) The part of the N-terminal mEH protein sequence encompassing the mEH membrane anchor. Positively and negatively charged amino acid residues are doubly and singly underlined respectively within a stretch of up to 15 amino acid residues on each side of the hydrophobic core sequence of the membrane anchor. Residues that have been mutated for the generation of $^{++}$mEH (positions 2 and 4) and mEH_{g1} (positions 39 and 40) are numbered.

MATERIALS AND METHODS

Construction of templates

The cDNA coding for the rat mEH was a gift from C. B. Kasper [21]. The construction of the template coding for an mEH without a membrane anchor (δmEH) has been described [9].

To change the net charge of the N-terminus of mEH by $Trp^2 \rightarrow Arg$ and $Glu^4 \rightarrow Lys$ mutations, mEH cDNA was modified as follows (see Figure 1). MEH cDNA was amplified by PCR with the mutagenic oligomer 1a (5′-TCCCTGCTGCA-GTCAGGAGTCATG**C**GGCTG**A**AAC) and the oligomer 1b (5′-CTCATAGAAGGATCCAGG). Primer 1a includes the mEH initiation codon for protein biosynthesis (underlined nucleotides), two mismatches with the template DNA (bold nucleotides) and covers a *Pst*I site in the 5′ untranslated region of the mEH cDNA. The primer 1b extends across the unique *Bam*HI site of the mEH cDNA. The amplified DNA was restricted with *Pst*I and *Bam*HI and inserted into the plasmid pSP65EHE/B containing the 5′ *Eco*RI–*Bam*HI restriction fragment of the mEH cDNA, to replace the analogous *Pst*I–*Bam*HI fragment in the mEH cDNA. From the resulting clone, the *Eco*RI–*Bam*HI fragment was used to replace the analogous fragment in the full-length mEH cDNA to yield the template for $^{++}$mEH (mEH in which charges in the N-terminal sequence have been altered by +3). The correct sequence of the $^{++}$mEH template was verified by DNA sequencing.

A glycosylation site in mEH was created by $Lys^{39} \rightarrow Asn$ and $Pro^{40} \rightarrow Ala$ residue replacements as follows. The mEH cDNA was amplified by using primer pair 2a (5′-CCGGAATTCTGG-GAGGAACCAGGGCCTAC) and 2b (5′-TTTGGCTGAT-G**CA**TTTGACCCTGG), and in a separate reaction by primer pair 2c (5′-CCAGGGTCAAA**TG**CATCAGCCAAAG) and 1b. Primer 2a contains an extraneous *Eco*RI recognition sequence. The mutant primers 2b and 2c are partly complementary to each other and contain two mismatches to the mEH cDNA (bold nucleotides) creating a *Nsi*I site in the resulting PCR products. The PCR products of the reactions with primers 2a and 2b as well as with primers 2c and 1b were restricted with *Eco*RI–*Nsi*I and *Bam*HI–*Nsi*I respectively. Both fragments were used in a trimolecular ligation reaction to replace the analogous *Eco*RI–*Bam*HI fragment in the mEH cDNA to yield the template coding for mEH with the introduced glycosylation signal. This construct was termed mEH_{g1}.

In addition we generated a cDNA coding for an mEH, termed mEH_{g2}, with a more C-terminally located glycosylation site by $Gln^{303} \rightarrow Asn$ mutation. The strategy used for the construction of this template relied on a published method for site-directed mutagenesis by PCR [22]. The site selected for site-directed mutagenesis was flanked by two *Stu*I sites. PCR was performed in two separate reactions. Reaction 1 included primers 3a (5′-CCAACCACGTGAAAGGCCTGCAC) and 3b (5′-CC-GAAGACCTTGGTGGC**AT**TGATGTGTAAG). Reaction 2 included primers 3c (5′-CCGAAGACCCACCAAGCCAGAC-ACTG) and 3d (5′-AACTTCCTCTCCAGGCCTCC). Primers 3a and 3d cover the 5′ and the 3′ *Stu*I sites of the mEH cDNA respectively. Primers 3b and 3c are partly complementary to mEH and to each other. Primer 3b contains the mutagenic mismatches (bold). Both primers contain an extraneous *Bbs*I recognition site (underlined). After PCR both reaction products were digested with *Stu*I and *Bbs*I and used to replace the analogous fragments in the mEH cDNA.

For engineering single glycosylation signals into two regions of the $^{++}$mEH template, a *Sma*I–*Sal*I or a *Bam*HI–*Sal*I restriction fragment was isolated from the mEH_{g1} or mEH_{g2} cDNA species respectively (see Figure 1). These fragments were used to replace the analogous fragments in $^{++}$mEH to yield the templates coding for $^{++}mEH_{g1}$ and $^{++}mEH_{g2}$.

For heterologous expression in COS cells, the modified mEH cDNA constructs were cloned into the vector pcDNA I/Amp (Invitrogen).

Expression and analysis of recombinant protein

Protein concentrations were determined by the Bradford assay as described by the manufacturer (Bio-Rad). Translation of mEH and δmEH *in vitro* in the presence of dog pancreas microsomes was performed as described [9]. For transient expression of the various mEH constructs, COS 7 cells were transfected by using the DEAE-dextran method in the presence of chloroquine [23]. For small-scale experiments 150 ng of DNA was transfected per 20000 seeded COS 7 cells. For experiments requiring a larger number of cells (e.g. determination of enzyme activities), 6 μg of DNA was transfected into 5×10^5 cells. The cells were incubated for 4 h with the DNA/DEAE-dextran mixture, washed with PBS containing 10% (v/v) DMSO and incubated for 3–4 days in Dulbecco's modified Eagle's medium (DMEM) containing 10% (v/v) fetal calf serum. The cells were trypsinized and washed with DMEM containing 10% (v/v) fetal calf serum and resuspended in cell buffer [0.1 M Tris/HCl, pH 9.0, 20% (v/v) glycerol, 2 trypsin inhibitor units/ml aprotinin and 0.5 mM PMSF]. The cells were disrupted by ultrasonication with a Branson ultrasonifier with a fitted microtip head (output 5, 10% duty cycle, ten pulses) for further analysis.

Total cellular membranes were isolated from the cellular homogenate by centrifugation at 150000 ***g*** for 15 min in an Airfuge and, depending on the recombinant protein expressed, 20 or 100 μg of the membrane fraction was treated with 0.5 or 2 m-units respectively of endoglycosidase H (endo H), as described [24], for 5.5 h. The assay mixture was analysed by SDS/PAGE followed by immunoblotting [25] using as the first antibody a polyclonal antiserum directed against rat mEH.

For the alkaline extraction assay, cellular lysate was prepared from COS cells as described above and centrifuged at 5000 ***g*** for 10 min. The resulting supernatant (total 10–50 μg of protein depending on the cellular content of the recombinant protein analysed) was diluted 1:10 with 0.1 M Na_2CO_3, pH 11.5, and left on ice for 15 min. The incubation mixture was layered on top of an equal volume of an alkaline sucrose cushion [26]. Protein was concentrated from the resulting supernatant by precipitation with trichloroacetic acid, followed by washing with 80% (v/v) ethanol. The pellet and the supernatant of the alkaline extraction assay were analysed by SDS/PAGE followed by immunoblotting as described above.

For the determination of the cellular mEH enzyme activity, cellular lysate was prepared as described above. The enzyme activity of the lysed cells towards benzo[*a*]pyrene 4,5-oxide was assayed with approx. 100 μg of cellular protein for 30 min [27,28]. Under these conditions the enzyme activity was linear with time and protein.

RESULTS

The N-terminal amino acid sequence of the rat mEH is shown in Figure 1(B). In the topogenic region [11] this sequence contains, as well as the positively charged N-terminus, one negatively charged amino acid residue at position 4, followed by a hydrophobic core of 16 residues. This core precedes a stretch of 15 residues containing two positively and four negatively charged amino acids, followed by the remaining peptide chain. To obtain a mutant mEH protein with a high probability of adopting a type II membrane topology [29], we changed the net charge of the mEH N-terminus by +3, resulting in the protein $^{++}$mEH.

For the investigation of the membrane orientation of mEH and $^{++}$mEH, we wished to make use of the observation that proteins that are exposed to the lumen of the ER can become N-glycosylated provided that the peptide chain contains a potential N-glycosylation signal. Because this is not true of mEH or

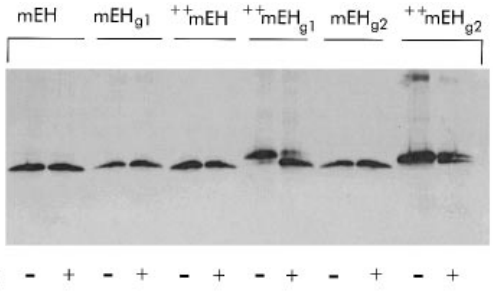

Figure 2 N-glycosylation analysis of the mEH and modified mEH proteins

The mEH and modified mEH proteins were transiently expressed in COS cells and endo H treated (+) or untreated (−) cellular lysates derived from these cells were analysed by immunoblotting, using as the first antibody a polyclonal antiserum directed against rat mEH. The blot was developed with the enhanced chemiluminescence system (Amersham).

$^{++}$mEH, this signal was generated by mutagenizing $Lys^{39}Pro^{40}Ser^{41}$ of both proteins to $Asn^{39}Ala^{40}Ser^{41}$, yielding the proteins mEH$_{g1}$ and $^{++}$mEH$_{g1}$. To exclude the remote possibility that these mutations might affect the mEH topology owing to their neighbourhood to the membrane anchor, we generated a second set of mEH and $^{++}$mEH constructs containing a glycosylation site in the middle of the peptide chain. This was performed by mutagenizing $Gln^{303}Ala^{304}Thr^{305}$ to $Asn^{303}Ala^{304}Thr^{305}$, yielding the proteins mEH$_{g2}$ and $^{++}$mEH$_{g2}$.

The modified mEH proteins were transiently expressed in COS cells to analyse for N-glycosylation. The total cellular COS protein was subjected to immunoblotting, using as the first antibody an antiserum directed against the rat mEH (Figure 2). Cellular protein isolated from non-transfected COS cells did not yield any immunodetectable protein (results not shown). Protein isolated from cells transfected with the cDNA coding for the modified mEH proteins contained large amounts of immunoreactive protein. Transiently expressed mEH and $^{++}$mEH, which do not contain a glycosylation signal, as well as mEH$_{g1}$ and mEH$_{g2}$, had the same mobility. Endo H treatment did not alter the mobilities of mEH and mutant mEH proteins. However, altering the N-terminal charge of mEH$_{g1}$ and mEH$_{g2}$ by +3 resulted in glycosylation, as evidenced by the lower mobilities of $^{++}$mEH$_{g1}$ and $^{++}$mEH$_{g2}$ than mEH$_{g1}$ and mEH$_{g2}$. Treatment of $^{++}$mEH$_{g1}$ and $^{++}$mEH$_{g2}$ with endo H increased the mobilities of these proteins to those of mEH$_{g1}$ and mEH$_{g2}$. However, the $^{++}$mEH$_{g2}$ was partly resistant to digestion with endo H. Taken together, these results demonstrate that the potential glycosylation sites were glycosylated in $^{++}$mEH$_{g1}$ and $^{++}$mEH$_{g2}$, which therefore have a type II membrane topology. However, these sites are not used in mEH$_{g1}$ and mEH$_{g2}$, which consequently display a type I topology. Altering the net charge of the mEH N-terminus to more positive values is sufficient to invert the mEH membrane topology. The sensitivity of $^{++}$mEH$_{g1}$ to endo H indicates that, like mEH, this protein is retained in the ER.

The membrane association of mEH and the modified mEH proteins was analysed by alkaline extraction of total cellular protein of COS cells expressing these proteins (Figure 3A). As expected from previous results [9], mEH, which is an integral membrane protein, was resistant to alkaline extraction. Addition of a glycosylation site to mEH, resulting in the protein mEH$_{g1}$, did not change this property. Similarly $^{++}$mEH$_{g1}$ is an integral membrane protein as shown by its resistance to alkaline membrane extraction. However, under these conditions mEH with a deleted membrane anchor, termed δmEH, which has been shown

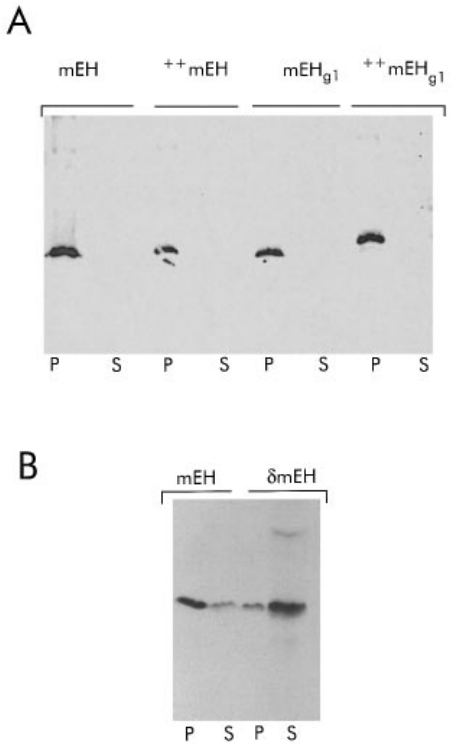

Figure 3 Membrane integration assay of the mEH and modified mEH proteins

(**A**) Cellular membranes derived from cells expressing the recombinant mEH proteins were alkali-extracted and centrifuged as described in the text. The resulting pellets (P) and supernatants (S) were analysed by immunoblotting as described in the legend to Figure 2. (**B**) For validation of the assay, mEH and δmEH, which is a peripheral membrane protein [9], were translated *in vitro* in the presence of dog pancreas microsomes and [^{35}S]methionine. The microsomes were mixed with cellular membranes from non-transfected COS cells and assayed by alkaline extraction. The resulting fractions were analysed by SDS/PAGE followed by fluorography.

Table 1 Enzyme activity, relative expression level and relative enzyme activities of mEH_{g1} and $^{++}mEH_{g1}$ in cellular membranes

The two engineered mEH proteins were transiently expressed in COS cells. The cells were lysed by ultrasonication, and membranes were prepared from the resulting lysate as described in the Materials and methods section. The mEH enzyme activity towards benzo[*a*]pyrene 4,5-oxide was determined in membranes derived from COS cells and from cells expressing the two mEH-related proteins. The enzyme activity was determined in four independent experiments. For the analysis of the relative expression level, immunoreactive mEH protein was detected by immunoblotting and the resulting signal was quantified densitometrically. Two different amounts (0.5 and 1 μg) of membranes derived from one transfection were analysed to ensure linearity of the resulting signal. The resulting values differed from the means by less than 10%. Relative enzyme activity was calculated from the mEH enzyme activity obtained for the two heterologously expressed proteins after subtraction of the enzyme activity obtained for COS cells and taking into account their relative expression levels. Abbreviations: n.d., not detectable; n.a., not available.

Protein expressed	Enzyme activity (pmol/min per mg of protein)	Expression level*	Relative enzyme activity (%)
None	7 ± 2	n.d.	n.a.
mEH_{g1}	195 ± 47	228	100
$^{++}mEH_{g1}$	46 ± 7	83	55

* Arbitrary units.

to be a peripherally associated membrane protein [9] and which we were not able to express in COS cells, is extracted from a mixture of dog pancreas microsomes containing δmEH translated *in vitro*, as well as cellular membranes derived from non-transfected COS cells (Figure 3B). On the basis of the results of the alkaline-extraction assay of the modified mEH proteins, we conclude that the anchoring function of the mEH membrane-anchor signal sequence is maintained on topological inversion of mEH.

The enzyme activity of mEH_{g1} and $^{++}mEH_{g1}$ towards benzo[*a*]pyrene 4,5-oxide was evaluated in cellular extracts and the relative expression levels of the recombinant proteins were determined by immunoblotting followed by densitometric quantification of the signals (Table 1). From these results the relative catalytic-centre activities of these enzymes were calculated. It was found that cells transfected with the cDNA constructs coding for either mEH_{g1} or $^{++}mEH_{g1}$ had a 28-fold and a 7-fold respectively higher enzyme activity than the untransfected COS cells. However the relative catalytic-centre activities calculated for mEH_{g1} and $^{++}mEH_{g1}$ differed by less than a factor of two. From these results we conclude that the topological inversion of mEH has only a moderate effect on the catalytic properties of the enzyme.

DISCUSSION

The role of the membrane topology of a set of enzymes catalysing a metabolic cascade has not yet been established. Cytochrome *P*-450 and mEH catalyse a metabolic cascade resulting in the formation of the ultimate carcinogenic metabolites of polycyclic aromatic hydrocarbons. It has been well documented that cytochrome *P*-450 has an N-terminal membrane anchor and assumes a type I membrane topology in the ER [29–31]. The orientation of the cytochrome *P*-450 membrane anchor can be inverted by changing the net charge of the peptide sequence preceding the hydrophobic core of the membrane anchor to more positive values [29,31]. However, the consequences of topological inversion on the catalytic activity of cytochrome *P*-450 have not been evaluated because it is highly likely that they would eliminate cytochrome *P*-450 function, at least because cytochrome *P*-450 reductase, which is exposed to the cytosolic side of the ER, might not couple with the luminal cytochrome *P*-450. The requirements for the catalytic activity of mEH are less stringent as this protein does not contain a prosthetic group and uses water as a cosubstrate. We therefore decided to invert the membrane topology of mEH as an important step in the evaluation of the resulting toxicological consequences. In the course of these studies we have firmly established the mEH membrane topology, which until now has been disputed [13,14,17].

For this purpose we changed the total charge of the mEH peptide sequence preceding the hydrophobic core of the recently identified membrane anchor [9] by +3, resulting in $^{++}$mEH. Initially we tried to investigate the membrane topology of mEH and $^{++}$mEH transcribed and translated *in vitro* by using protease protection assays of co-translationally added dog pancreas microsomes. However, using this approach we found that mEH, which had been synthesized in the absence of dog pancreas microsomes, was already extremely resistant to digestion by several proteases, and co-translational addition of microsomes did not change this protease protection pattern. This finding agrees with the results of others that even the purified mEH was resistant to digestion by several proteases unless detergent was added [13].

N-glycosylation of membrane proteins has, however, provided a powerful tool in the study of their topology. Because mEH and $^{++}$mEH are lacking a natural N-glycosylation site, it was engineered into the peptide chain at a position located 19 residues after the termination of the hydrophobic part of the membrane anchor. The rationale for selecting this location was that it is outside the region of the membrane anchor, which is involved in determining the topology of membrane proteins [11,12]. In addition, mutagenesis in this region should not interfere with the catalytic activity of mEH as this part of mEH is not highly conserved between rat, human and rabbit mEH and is distant from the putative catalytic centres of mEH, which are located in the region of residues 200–435 [32,33]. In a second construct, an N-glycosylation site was engineered at amino acid residue 303, resulting in the construct mEH_{g2}.

Our results show that only glycosylation sites engineered into $^{++}$mEH (i.e. $^{++}mEH_{g1}$ and $^{++}mEH_{g2}$), for which the charge difference, δ(C-N), is -5, become glycosylated whereas the same glycosylation sites engineered into mEH (i.e. mEH_{g1} and mEH_{g2}) are not utilized (Figure 2). This result clearly demonstrates that the mEH when expressed in fibroblasts has a type I topology, despite having a δ(C-N) of -2 in the membrane anchor, which according to the algorithm by Hartman et al. [11] would predict a type II membrane topology for mEH. The topology of mEH and $^{++}$mEH is, however, correctly predicted by the 'positive inside' rule, which states that membrane anchors orient themselves in the membrane in such a way that the end containing most positively charged residues faces the cytosolic face of the membrane [34]. In mEH, positively charged residues are, with the exception of the positively charged N-terminal methionine residue, located only at the C-terminal side of the membrane anchor. Our results do not support recent experimental evidence on the mEH membrane topology in hepatocytes. In those studies it was shown that certain mEH epitopes are partly inaccessible to a subset of monoclonal antibodies [16]. On the basis of these studies it was suggested that mEH can assume a type I as well as a type II topology. Although we cannot exclude the possibility that the mEH membrane topology in hepatocytes and fibroblasts is different, our results agree with mEH topology models suggested earlier, based on immuno-electronmicroscopy [14] or on experiments with membrane-impermeant fluorescent probes [13]. Because mEH and cytochrome *P*-450 have the same membrane topologies they should display a higher probability of physical interaction than in a model that places both proteins on opposite sides of the membrane. In fact, a physical interaction of cytochrome *P*-450 and mEH has been shown by using rotational diffusion analysis [35].

In addition, the sensitivity of $^{++}mEH_{g1}$ to endo H (Figure 2) indicates that ER-retention signal(s) in mEH, as yet unidentified, remain functional on topological inversion of the protein. Glycosylation of $^{++}mEH_{g2}$ might have interfered with the retention of this protein in the ER as it was partly resistant to treatment with endo H.

Metabolic channelling catalysed by cytochrome *P*-450 and mEH on the same side of the membrane should lead to a highly efficient formation of the ultimate carcinogenic dihydrodiol epoxides from polycyclic aromatic hydrocarbons. This hypothesis could be tested by topological inversion of mEH provided that the resulting enzyme was still an integral membrane protein and retained its catalytic activity. The feasibility of this approach is evident from our finding that mEH_{g1} and $^{++}mEH_{g1}$ are both integral membrane proteins with opposite membrane topologies, and display similar turnover numbers towards the mutagenic metabolite benzo[*a*]pyrene 4,5-oxide, which is formed by the action of cytochrome *P*-450 in the liver.

Simultaneously our results demonstrate for the first time that it is feasible to invert the topology of an integral membrane protein with only moderate effects on its catalytic activity, despite the different folding environments that have been found on each side of membranes [36]. Different topologies of mEH might also be found in different species. In this respect it is interesting to note that an mEH from the tobacco moth, *Manduca sexta*, which hydrolyses epoxide-containing sesquiterpene ester juvenile hormones [37], might adopt a type II membrane topology. This protein resembles the $^{++}$mEH described in the present study because in the insect mEH a positively charged lysine precedes the hydrophobic core of the membrane anchor, which at its C-terminal side is mainly negatively charged.

We thank Dr. C. B. Kasper for the gift of mEH cDNA, and Mrs. Irmgard Ihrig-Biedert for excellent technical support. This work was supported by the German Research Council (DFG) (SFB302-A70).

REFERENCES

1 Oesch, F. (1973) Xenobiotica **3**, 305–340
2 Grover, P. L. (1986) Xenobiotica **16**, 915–931
3 Davies, R. L., Crespi, C. L., Rudo, K., Turner, T. R. and Langenbach, R. (1989) Carcinogenesis **10**, 885–891
4 Wood, A. W., Levin, W., Lu, A. Y. H., Yagi, H., Hernandez, O., Jerina, D. M. and Conney, A. H. (1976) J. Biol. Chem. **251**, 4882–4890
5 Sharma, R. N., Gurtoo, H. L., Farber, E., Murray, R. K. and Cameron, R. G. (1981) Cancer Res. **43**, 3311–3319
6 Gonzalez, F. J. and Kasper, C. B. (1980) Biochem. Biophys. Res. Commun. **93**, 1254–1258
7 Okada, Y., Frey, A. B., Guenthner, T. M., Oesch, F., Sabatini, D. D. and Kreibich, G. (1982) Eur. J. Biochem. **122**, 393–402
8 Galteau, M. M., Antoine, B. and Reggio, H. (1985) EMBO J. **4**, 2793–2800
9 Friedberg, T., Löllmann, B., Becker, R., Holler, R. and Oesch, F. (1994) Biochem. J. **303**, 967–972
10 Sabatini, D. D. and Adesnik, M. B. (1995) in The Metabolic Basis of Inherited Disease, vol. 1 (Scriver, C. R., Beaudet, A. L., Sly, W. S. and Valle, D., eds.), pp. 459–553, McGraw-Hill, New York
11 Hartman, E., Rapoport, T. A. and Lodish, H. F. (1989) Proc. Natl. Acad. Sci. U.S.A. **86**, 5786–5790
12 Beltzer, J. P., Fiedler, K., Fuhrer, C., Geffen, I., Handschin, C., Wessels, H. P. and Spiess, M. (1991) J. Biol. Chem. **266**, 973–978
13 Craft, J. A., Baird, S., Lamont, M. and Burchell, B. (1990) Biochim. Biophys. Acta **1046**, 32–39
14 Waechter, F., Bentley, P., German, M., Oesch, F. and Stäubli, W. (1982) Biochem. J. **202**, 677–686
15 Welch, G. R. and Easterby, J. S. (1994) Trends Biochem. Sci. **19**, 193–197
16 Alves, C., Von Dippe, P., Amoui, M. and Levy, D. (1993) J. Biol. Chem. **268**, 20148–20155
17 von Dippe, P., Amoui, M., Alves, C. and Levy, D. (1993) Am. J. Physiol. **264**, G528–G534
18 Honscha, W., Platt, H. D., Oesch, F. and Friedberg, T. (1995) Biochem. J. **311**, 975–979
19 Bergeron, J. J. M., Brenner, M., Thomas, D. Y. and Williams, D. B. (1994) Trends Biochem. Sci. **19**, 124–128
20 Freedman, R. B., Hirst, T. and Tuite, M. F. (1994) Trends Biochem. Sci. **19**, 331–336
21 Porter, T. D., Beck, T. W. and Kasper, C. B. (1986) Arch. Biochem. Biophys. **248**, 121–129
22 Tomic, M., Sunjevaric, I., Savtchenkov, E. S. and Blumenberg, M. (1990) Nucleic Acids Res. **18**, 1656
23 Clark, B. J. and Waterman, M. R. (1991) Methods Enzymol. **207**, 100–108
24 Szczesna-Skorupa, E. and Kemper, B. (1993) J. Biol. Chem. **268**, 1757–1762
25 Steinberg, P., Lafranconi, M., Wolf, C. R., Waxman, D. J., Oesch, F. and Friedberg, T. (1987) Mol. Pharmacol. **32**, 463–470
26 Szczesna-Skorupa, E. and Kemper, B. (1991) Methods Enzymol. **207**, 64–75
27 Glatt, H. R., Kaltenbach, E. and Oesch, F. (1980) Cancer Res. **40**, 2552–2553
28 Schmassmann, H. U., Glatt, H. R. and Oesch, F. (1976) Anal. Biochem. **74**, 94–104
29 Szczesna-Skorupa, E., Browne, N., Mead, D. and Kemper, B. (1988) Proc. Natl. Acad. Sci. U.S.A. **85**, 738–742
30 Monier, S., van Luc, P., Kreibich, G., Sabatini, D. D. and Adesnik, M. (1988) J. Cell Biol. **107**, 457–470
31 Sakaguchi, M., Tomiyoshi, R., Kurigawa, T., Mihara, K. and Omura, T. (1992) Proc. Natl. Acad. Sci. U.S.A. **89**, 16–19

32 Arand, M., Grant, D. F., Beetham, J. K., Friedberg, T., Oesch, F. and Hammock, B. D. (1994) FEBS Lett. **338**, 251–256
33 Lacouciere, G. M. and Armstrong, R. N. (1993) J. Am. Chem. Soc. **115**, 10466–10467
34 von Heijne, G. (1989) Nature (London) **341**, 456–458
35 Etter, H. U., Richter, C., Ohta, Y., Winterhalter, K. H., Sasabe, H. and Kawato, S. (1991) J. Biol. Chem. **266**, 18600–18605
36 Gething, M. J. and Sambrook, J. (1992) Nature (London) **355**, 33–45
37 Wojtasek, H. and Prestwich, G. D. (1996) Biochem. Biophys. Res. Commun. **220**, 323–329

Received 24 April 1996; accepted 29 May 1996